Acta Cryst. (1980). A**36**, 282–287

The Significance of the Radial Autocorrelation Function for the Interpretation of Equatorial Diffraction from Biological Membranes

BY MIKIO KATAOKA AND TATZUO UEKI

Department of Biophysical Engineering, Faculty of Engineering Science, Osaka University, Toyonaka, 560, Japan

(*Received* 28 *June* 1979; *accepted* 18 *October* 1979)

Abstract

Oriented specimens of biomembranes give distinct X-ray diffraction patterns of circular symmetry along the equatorial plane. In order to interpret such a diffraction pattern, properties of the radial autocorrelation function were examined in detail in conjunction with electron-density distribution and applied. The radial autocorrelation function, which is the Fourier–Bessel transform of an intensity function with circular symmetry, is the radial projection of a two-dimensional autocorrelation function and can be interpreted in terms of Fourier components of electron-density projection along the membrane normal. Some useful information is obtainable on the structure of the scatterer: (i) the approximate size of the X-ray scatterer; (ii) judgement of crystalline or non-crystalline arrangement of molecules; (iii) the existence of a regular arrangement of the electron-density fluctuations in a projection along the membrane normal; (iv) the rotational symmetry element existing in the scatterer if any.

Introduction

We have obtained continuous X-ray diffraction patterns in the equatorial direction from oriented specimens of some biomembranes; the outer membrane of *Salmonella typhimurium* and chromatophore from photosynthetic bacteria (Ueki, Kataoka & Mitsui, 1976). These patterns are caused by regular arrangements of protein molecules in the plane of the membranes. They consist of several diffraction maxima which are much sharper than the 'halo' from amorphous materials but broader than crystalline reflections. Although these maxima could be indexed on the basis of appropriate two-dimensional crystalline lattices (Ueki, Kataoka & Mitsui, 1976; Ueki, Mitsui & Nikaido, 1979), electron microscopic studies did not show any crystalline domains for these membranes. Therefore, we must find an effective and decisive method to interpret the equatorial diffraction patterns of these membranes.

Since the problem is concerned with the arrangement of protein molecules in X-ray scatterers, the Patterson function is relevant to our purpose. In crystal structure analysis, the Patterson function gives information on the space group (Buerger, 1959). In the case of membranes, X-ray scatterers are randomly rotated with respect to an axis normal to the membrane surface when they are stacked, and the equatorial intensity is a circular symmetric function depending only on the radial coordinate of the cylindrical polar coordinates. The Patterson function calculated from such a circular symmetrical intensity is called the 'radial autocorrelation function'. The cylindrically symmetrical Patterson function proposed for fibrous systems by MacGillavry & Bruins (1948), which is the same as the radial autocorrelation function in principle, has often been misunderstood to correspond to a cylindrically symmetric structure. However, it was used to preserve non-circular symmetric components of electron-density distribution in the scatterers even if directional components of vectors are lost (Earnshaw, Casjens & Harrison, 1976).

In this paper, we have developed a strict relation between the radial autocorrelation function and the electron-density distribution. We describe the usefulness of the radial autocorrelation function in the interpretation of diffraction patterns from protein assemblies in biomembranes through the model calculations for the arrangement of bacteriorhodopsin molecules which was given by Unwin & Henderson (1975). The equatorial diffraction pattern from the outer membrane was examined with the radial autocorrelation function.

I. Estimation of the radial autocorrelation function

I.1. *Fundamental equations*

In this paper, X-ray diffraction is discussed in terms of cylindrical polar coordinates. Two-dimensional vectors, (r,φ) and (R,Φ), are used in real and reciprocal space, respectively. Vector (u,χ) is used in vector space.

0567-7394/80/020282-06$01.00

We take a unique axis (z) of the membrane parallel to the membrane normal. An equatorial diffraction from the membrane corresponds mathematically to an electron-density projection along z. Thus, the X-ray scatterer which is related to the observed intensity, $I(R,\Phi,0)$, is the electron-density projection $\sigma(r,\varphi)$ of the protein assembly on the membrane matrix.

$$I(R,\Phi,0) = |\iiint \rho(r,\varphi,z) \exp[-2\pi i r R \cos(\varphi - \Phi)] \times r\,dr\,d\varphi\,dz|^2$$

$$= |\iint \sigma(r,\varphi) \exp[-2\pi i r R \cos(\varphi - \Phi)] \times r\,dr\,d\varphi|^2 \equiv I(R,\Phi), \quad (1)$$

where

$$\sigma(r,\varphi) = \int \rho(r,\varphi,z)\,dz.$$

In the X-ray specimens of biomembranes, all the rotational orientations of scatterers are equally probable about the z axis. Then, the observed equatorial intensity is a circular symmetrical function, $I_0(R)$, instead of $I(R,\Phi)$. $I_0(R)$ is obtained through the integration of $I(R,\Phi)$:

$$I_0(R) = \sum_n |F_n(R)|^2, \quad (2)$$

where

$$F_n(R) = \exp(-in\pi/2) \int \sigma_n(r) J_n(2\pi r R)\, 2\pi r\,dr. \quad (3)$$

J_n is the Bessel function of order n (Waser, 1955; Franklin & Klug, 1955). In the equation, $\sigma_n(r)$ is the Fourier coefficient in the expansion of $\sigma(r,\varphi)$ with respect to φ and is given by

$$\sigma_n(r) = \frac{1}{2\pi} \int \sigma(r,\varphi) \exp(in\varphi)\,d\varphi. \quad (4)$$

A radial autocorrelation function $A_0(u)$ is given by the inverse Fourier–Bessel transform of $I_0(R)$ (MacGillavry & Bruins, 1948):

$$A_0(u) = \int I_0(R) J_0(2\pi R u)\, 2\pi R\,dR. \quad (5)$$

It is important to point out that $A_0(u)$ is the first term in the Fourier expansion of $A(u,\chi)$ with respect to azimuth χ and is to be understood as the radial projection of $A(u,\chi)$. Therefore, $A_0(u)$ must be discussed on the basis of the two-dimensional autocorrelation function $A(u,\chi)$ of the structure in conjunction with the arrangement of molecules in the scatterer. In general, an electron-density projection, $\sigma(r,\varphi)$, can be expressed by summation of electron-density fluctuations. (As an example, the structure of a trimer of bacteriorhodopsin from purple membrane is shown in Fig. 1.) Vectors between fluctuations are represented by $A(u,\chi)$, that is, the disposition function of fluctuations determines the peak positions in $A(u,\chi)$ and thus $A_0(u)$. Especially in the case of crystals, the disposition function is a lattice function. We must have appreciable peaks in $A_0(u)$ which correspond to the vectors of the lattice points in a crystalline structure; for instance, if the equatorial diffraction pattern is from a two-dimensional hexagonal structure, we must observe large peaks at $u = a, \sqrt{3}a, 2a$ and so on (a being the cell edge).

I.2. *Radial autocorrelation function and electron-density fluctuation*

As was pointed out by MacGillavry & Bruins (1948), $A_0(u)$ is not calculated from the self-convolution of circular symmetrical electron density, $\sigma_0(r)$. This point can be clearly shown by the next equation which is derived from (2) and (5):

$$A_0(u) = \sum_n \int |F_n(R)|^2 J_0(2\pi R u)\, 2\pi R\,dR = \sum_n a_n(u). \quad (6)$$

Each $a_n(u)$ can be discussed on the basis of the Fourier components of electron-density fluctuation as follows.

In order to clarify the physical meaning, we represent the complex Fourier coefficient $\sigma_n(r)$ in terms of the modulus $|\sigma_n(r)|$ and phase $\alpha_n(r)$. Then, $\sigma(r,\varphi)$ can be expressed by (Vainshtein, 1966).

$$\sigma(r,\varphi) = \sigma_0(r) + 2 \sum_{n>0} |\sigma_n(r)| \cos[n\varphi + \alpha_n(r)]. \quad (7)$$

The nth component represents the electron-density fluctuation with n-fold rotational symmetry and its Fourier transform, $F'_n(R,\Phi)$, is related to $F_n(R)$ by (3) as

$$F'_n(R,\Phi) \equiv \mathcal{F}\{2|\sigma_n(r)| \cos[n\varphi + \alpha_n(r)]\} = \begin{cases} 2|F_n(R)| \cos[n\Phi + \beta_n(R)] & (n \text{ even}) \\ 2i|F_n(R)| \sin[n\Phi + \beta_n(R)], & (n \text{ odd}) \end{cases} \quad (8)$$

where $\mathcal{F}$ denotes the Fourier transform and $\beta_n(R)$ is the phase of $F_n(R)$. The Fourier transform of $|F'_n(R,\Phi)|^2$ is equal to the self-convolution of the n-fold rotational symmetrical component of $\sigma(r,\varphi)$ as is well known from the multiplication theorem of the Fourier integral.

$$\mathcal{F}[|F'_n(R,\Phi)|^2] = 2|\sigma_n(r)|^{\tilde{2}} \cos[n\varphi + \alpha_n(r)] = a'_n(u,\chi). \quad (9)$$

where $\tilde{2}$ denotes the self-convolution operation. $a'_n(u,\chi)$ is a two-dimensional function with $2n$-fold rotational symmetry given by

$$a'_n(u,\chi) = \begin{cases} 4\iint |F_n(R)|^2 \cos^2[n\Phi + \beta_n(R)] \times \exp[2\pi i R u \cos(\Phi - \chi)]\, R\,dR\,d\Phi \\ \qquad (n \text{ even}) \\ 4\iint |F_n(R)|^2 \sin^2[n\Phi + \beta_n(R)] \times \exp[2\pi i R u \cos(\Phi - \chi)]\, R\,dR\,d\Phi \\ \qquad (n \text{ odd}) \end{cases}$$

$$= 2(\int |F_n(R)|^2 J_0(2\pi Ru)\, 2\pi R\, dR + \mathrm{Re}\{\exp(i2n\chi) \int |F_n(R)|^2 \exp[i2\beta_n(R)] \times J_{2n}(2\pi Ru)\, 2\pi R\, dR\}). \quad (10)$$

On integration of (10) with respect to χ to obtain the radial projection of $a'_n(u,\chi)$, we have

$$\langle a'_n(u,\chi)\rangle_\chi = 2\int |F_n(R)|^2 J_0(2\pi Ru)\, 2\pi R\, dR = 2a_n(u).$$

$$a_n(u) = \tfrac{1}{2}\langle a'_n(u,\chi)\rangle_\chi. \quad (11)$$

Similarly, we can conclude that $a_{-n}(u)$ contributes to $\langle a'_n(u,\chi)\rangle_\chi$ as the other half component.

Equations (9) and (11) show that $a_n(u)$ is the radial autocorrelation function of the component with n-fold rotational symmetry of electron-density projection, $|\sigma_n(r)| \cos[n\varphi + \alpha_n(r)]$. $a_0(u)$ clearly corresponds to the circular symmetrical electron density $\sigma_0(r)$ and $a_n(u)$ includes information on the n-fold rotational symmetrical component. If we can extract the contributions of each $a_n(u)$ from $A_0(u)$, we may find the symmetry element of the X-ray scatterer.

I.3. *Analysis of radial autocorrelation function.*

We can extract useful clues for the structure of the scatterer from $A_0(u)$ as follows.

(i) The approximate size of the X-ray scatterer is easily estimated, if the scatterer is finite, from the region where $A_0(u)$ approaches zero (Porod, 1951).

(ii) Arrangement of constituent molecules: whether it is crystalline or not.

(iii) Fine structure in $A_0(u)$ shows explicitly the existence of electron-density fluctuations in the projected $\sigma(r,\varphi)$ along the z axis.

(iv) Fine structure in $A_0(u)$ suggests the regular arrangements of electron-density fluctuations such as rotational symmetry, because fine fringes in $A_0(u)$ suggest that the contribution of $a_n(u)$ is appreciable.

II. Estimation of $A_0(u)$ for arrangements of bacteriorhodopsin in purple membrane

The structure of the purple membrane was established by the filtering technique of electron micrographs (Unwin & Henderson, 1975). The essence of the structure is a two-dimensional hexagonal arrangement of trimers of protein, bacteriorhodopsin, with cell edge 62·7 Å. The trimer has a threefold rotational symmetry (Fig. 1). The monomer is composed of seven rod-like structures. The rods were found to be α-helices by X-ray diffraction (Henderson, 1975; Blaurock, 1975), and are approximately parallel to each other and parallel to the z axis.

Circular symmetrical intensity functions were calculated for the monomer and trimer by the formula given by Oster & Riley (1952). Fig. 2 shows intensity functions for the monomer and trimer of bacteriorhodopsin molecules, and the intensity for purple membrane which was taken from Henderson (1975).

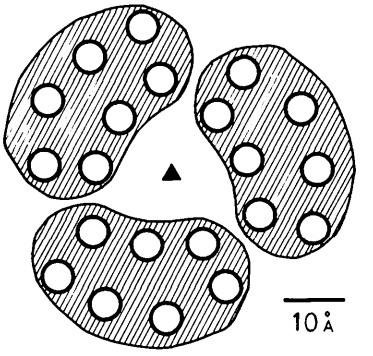

Fig. 1. Model structure of the trimer of bacteriorhodopsin projected along the z axis. The shaded regions show the monomers of bacteriorhodopsin which are arranged about a threefold rotational axis to form a trimer. The open circles show the seven α-helices (rods) which are parallel to each other. Rods have high electron density in the structure. The electron-density profile of a rod is approximated by an isotropic Gaussian function in the calculation of $I_0(R)$. When trimers are arranged according to a two-dimensional hexagonal lattice with $a = 62{\cdot}7$ Å, the structure of the purple membrane is formed. The original structure was presented by Unwin & Henderson (1975).

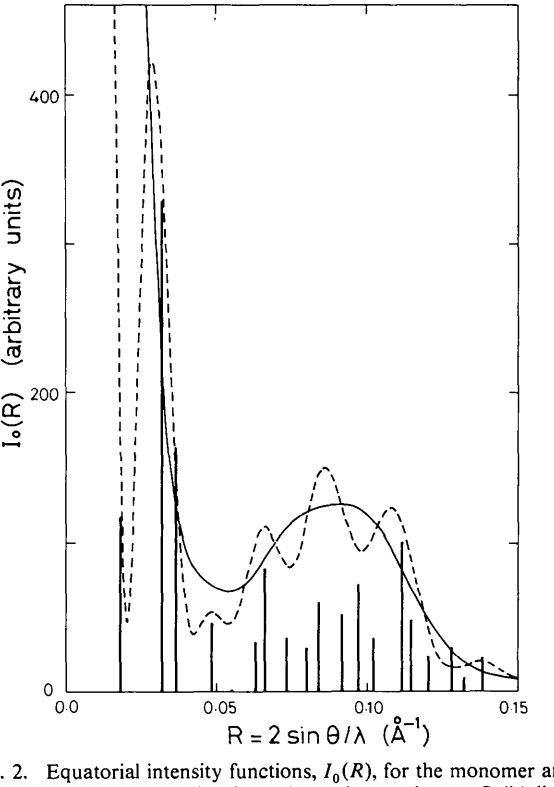

Fig. 2. Equatorial intensity functions, $I_0(R)$, for the monomer and trimer of bacteriorhodopsin and purple membrane. Solid line: monomer; broken line: trimer; vertical lines: Bragg reflections of purple membrane (taken from Henderson, 1975).

The monomer gives a continuous intensity function which has only one broad diffraction maximum at $d \simeq 10$ Å. The trimer apparently causes fine structure in the intensity profile. The broken line in Fig. 2 has similar features to the observed intensities from the outer membrane of *S. typhimurium* and chromatophore: broad but distinct diffraction maxima. Therefore, we can conclude that such a regular arrangement provides small- and moderate-angle diffraction patterns up to a spacing of 6–7 Å. Five maxima in the diffraction profile from the trimer can be indexed as a two-dimensional hexagonal lattice with $a = 80$ Å. This indexing is, of course, not meaningful, since the rods in the trimer have no crystalline arrangement, as is clear from Fig. 1. This fact indicates that indexing of a diffraction pattern may sometimes lead to incorrect conclusions for X-ray scatterers with such profiles. The intensity function for purple membrane consists of sharp Bragg reflections; they can be indexed as a two-dimensional hexagonal lattice with $a = 62{\cdot}7$ Å (Blaurock & Stoeckenius, 1971).

Radial autocorrelation functions calculated from the intensities in Fig. 2 are shown in Fig. 3. They correspond to the structures of monomer, trimer and purple membrane as below.

(i) $A_0(u)$'s for monomer and trimer decrease to zero at about 33 and 53 Å, in agreement with the sizes of the scatterers, while that for the purple membrane does not.

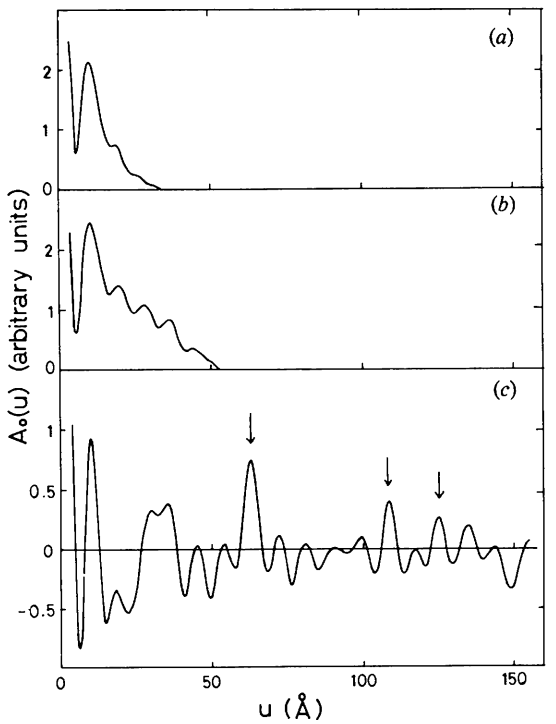

Fig. 3. Radial autocorrelation functions, $A_0(u)$, for (*a*) monomer, (*b*) trimer of bacteriorhodopsin and (*c*) purple membrane. Arrows in (*c*) indicate the expected positions of vectors from the two-dimensional hexagonal arrangement of trimers.

(ii) $A_0(u)$ for the purple membrane gives the peaks due to the two-dimensional hexagonal arrangement of trimers, at $u = 63$, 109, 126 Å, *etc.*, which correspond to the first, second, third, *etc.* neighbours in the lattice. In addition, there are peaks which come from the intra-trimer vectors. On the other hand, $A_0(u)$ for the trimer does not have peaks at $u = 80$ Å and so on, which must appear if the above-mentioned hexagonal lattice ($a = 80$ Å) is correct. Therefore, the indexing of the diffraction profile for the trimer is only by accident.

(iii) Fine structures of the first two can be interpreted on the basis of inter-rod distances (see Fig. 1). Peaks in $A_0(u)$ for the monomer reflect the intramolecular structure of the bacteriorhodopsin molecule, *i.e.* a peak at about 10 Å in $A_0(u)$ is from the nearest-neighbour distances of rods. The fact that no other appreciable peaks are observed in $A_0(u)$ for the monomer implies that there is no regular arrangement of rods in the molecule. $A_0(u)$ for the trimer gives information as to the intra- and inter-molecular vectors. The trimer gives more distinct peaks due to the regular arrangement of rods according to threefold rotational symmetry; the contribution of terms $a_n(u)$ to $A_0(u)$ in addition to $a_0(u)$ is appreciable, especially $a_3(u)$ and higher terms.

III. Interpretation of equatorial diffraction from outer membranes

We have found in-plane structural order in the outer membrane from *S. typhimurium* and chromatophore from photosynthetic bacteria (Ueki, Kataoka & Mitsui, 1976). Stacked membranes give diffuse but distinct X-ray diffraction in the equatorial direction. The equatorial diffraction pattern from the outer membrane was interpreted by means of a radial autocorrelation function.

The radial autocorrelation function of the outer membrane (see Fig. 3 of Ueki, Mitsui & Nikaido, 1979) reveals features of the protein assemblies as follows.

(i) The size of the scatterer is estimated to be about 100 Å at the most.

(ii) Although the equatorial reflections can be indexed as a two-dimensional hexagonal lattice with $a = 80$ Å (Ueki, Mitsui & Nikaido, 1979), $A_0(u)$ does not have the peaks expected from the assumed lattice. Therefore, the indexing is concluded to be accidental. This result is consistent with the electron microscopic study (Smit, Kamio & Nikaido, 1976).

(iii) Fine structure in $A_0(u)$ indicates the existence of fluctuations in the projected electron-density distribution.

(iv) Arrangement of the fluctuations has a regularity other than crystalline order (see *Discussion*).

Discussion

The results in the former sections showed that indexing of intensity maxima sometimes led to erroneous conclusions for the arrangement of molecules in an assembly with finite size. In such scattering systems, we found that the radial autocorrelation function, $A_0(u)$, provided useful information about the structure of the scatterer.

Although $A_0(u)$ is directly derived from the observed intensity function without any assumption, there are two problems encountered in the analysis of such a system; one is the background subtraction to obtain an intensity function from the experimental data and the other is the truncation effect.

We have examined the effects of background subtraction on $A_0(u)$ by using intensity functions from the outer membrane and chromatophore. By various estimations of background level, $I_0(R)$'s were obtained and were transformed into $A_0(u)$'s. The results indicated that peak positions of vector magnitudes in $A_0(u)$ were not influenced appreciably (the shifts are only 0·5–1·0 Å) by different background levels, but peak heights changed considerably. In the approach of the radial autocorrelation function presented in this paper, we utilized peak positions and were not concerned with quantitative analysis of peak heights. Therefore, the above discussion is not influenced by the ambiguity of background subtraction.

As for the truncation effect, peak positions in $A_0(u)$ are little influenced, except for a small u region, as a result of the calculations of model structures. Thus, the above discussion is also valid if $A_0(u)$ is calculated through $I_0(R)$ at the resolution of about 7 Å.

Provided that we have intensity data with sufficient accuracy and can also estimate the background level with reliability, we can perform a more quantitative analysis of the radial autocorrelation function. As is clear from (6), if we can estimate each $a_n(u)$ from $A_0(u)$, the radial autocorrelation function is a powerful technique for the structure analysis. How is $a_n(u)$ estimated? Firstly, we estimate a function $[A_0(u) - a_0(u)]$ by drawing a mean curve through $A_0(u)$, and this function corresponds to

$$[A_0(u) - a_0(u)] = \sum_{n \neq 0} a_n(u).$$

In the equation, $a_n(u)$ can be discussed on the basis of the nth Fourier component of electron-density fluctuation and its autocorrelation function, as is discussed in the former section; for $n = 1$, the structure is of a dipole arrangement, for $n = 2$, the arrangement is quadrupole and so on. These arrangements of electron-density fluctuations give characteristic vectors in $A(u,\chi)$ and hence vector magnitudes in $A_0(u)$ (see Fig. 4). For instance, if we can find a minimum at r_0 and a maximum at $\sqrt{2}r_0$ in $A_0(u)$, these peaks suggest an arrangement of electron-density fluctuations with $n = 2$, and if we find two minima at r_0 and $2r_0$ and one positive maximum at $\sqrt{3}r_0$, an arrangement of electron-density fluctuations with $n = 3$ is predicted. In Fig. 4, the above-mentioned cases are depicted schematically.

Thus, we can find the Fourier components of electron-density fluctuations by way of the radial autocorrelation function. Especially when the scatterer has rotational symmetry, the method of radial autocorrelation function will be quite effective for structure analysis.

In the case of the outer membrane, we did not know the background level with sufficient accuracy so we did not have any conclusive results from the procedure mentioned above. However, we could still suggest relations between the peak positions in $A_0(u)$; $n = 3$ seemed to be best-fitted. The electron microscopic study on the outer membrane from *Escherichia coli* suggested that the protein assembly had threefold rotational symmetry (Steven, Heggeler, Miller, Kistler & Rosenbusch, 1977). Since the X-ray diffraction pattern from the outer membrane of *S. typhimurium*

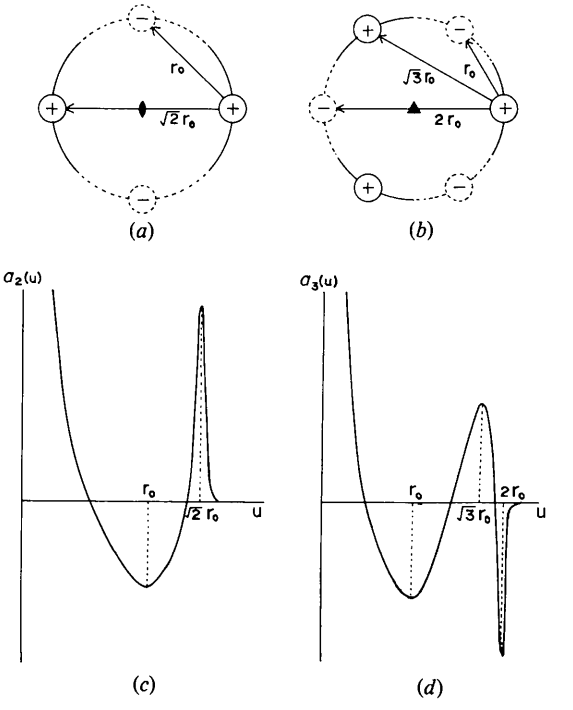

Fig. 4. Schematic picture of $|\sigma_n(r)| \cos(n\varphi)$ with (*a*) $n = 2$ and (*b*) $n = 3$, and corresponding (*c*) $a_2(u)$ and (*d*) $a_3(u)$. Solid line of (*a*) and (*b*) indicates positive and broken line negative values. Symbols + and − represent maximum and minimum, respectively. High electron-density regions are located on the circle with two- or three-fold rotational symmetry and the second or the third Fourier component of the electron-density fluctuations is shown as (*a*) or (*b*). The maxima and minima in (*c*) or (*d*) correspond to the magnitude of vectors indicated in (*a*) or (*b*), respectively.

resembles very much that of *E. coli* (Ueki, Tanaka, Nakae & Nikaido, 1979), the agreement of the results from X-ray and electron microscopy indicates that the interpretation of $A_0(u)$ is correct. The model construction of the protein assembly from $A_0(u)$ with threefold rotational symmetry was carried out and we have obtained a reasonable model structure of the assembly (Ueki, Tanaka & Nakae, 1979).

For the equatorial diffraction from chromatophore of *Rhodospirillum rubrum*, the method using the radial autocorrelation function was applied. Although we have reported that equatorial reflections could be indexed as a two-dimensional hexagonal lattice with $a = 42{\cdot}6$ Å (Ueki, Kataoka & Mitsui, 1976), the radial autocorrelation function suggests that the protein assembly is not crystalline but has rotational symmetry. Details will be published elsewhere (Kataoka & Ueki, 1979).

References

BLAUROCK, A. E. (1975). *J. Mol. Biol.* **93**, 139–158.

BLAUROCK, A. E. & STOECKENIUS, W. (1971). *Nature (London) New Biol.* **233**, 152–155.

BUERGER, M. J. (1959). *Vector Space and its Application in Crystal-Structure Investigation.* New York: John Wiley.

EARNSHAW, W., CASJENS, S. & HARRISON, S. C. (1976). *J. Mol. Biol.* **104**, 387–410.

FRANKLIN, R. E. & KLUG, A. (1955). *Acta Cryst.* **8**, 777–780.

HENDERSON, R. (1975). *J. Mol. Biol.* **93**, 123–138.

KATAOKA, M. & UEKI, T. (1979). In preparation.

MACGILLAVRY, C. H. & BRUINS, E. M. (1948). *Acta Cryst.* **1**, 156–158.

OSTER, G. & RILEY, D. P. (1952). *Acta Cryst.* **5**, 272–276.

POROD, G. (1951). *Kolloid Z.* **124**, 83–114.

SMIT, J., KAMIO, Y. & NIKAIDO, H. (1976). *J. Bacteriol.* **124**, 942–958.

STEVEN, A. C., HEGGELER, B., MILLER, R., KISTLER, J. & ROSENBUSCH, J. P. (1977). *J. Cell Biol.* **72**, 292–301.

UEKI, T., KATAOKA, M. & MITSUI, T. (1976). *Nature (London)*, **262**, 809–810.

UEKI, T., MITSUI, T. & NIKAIDO, H. (1979). *J. Biochem. (Tokyo)*, **85**, 173–182.

UEKI, T., TANAKA, M. & NAKAE, T. (1979). In preparation.

UEKI, T., TANAKA, M., NAKAE, T. & NIKAIDO, H. (1979). In preparation.

UNWIN, P. N. T. & HENDERSON, R. (1975). *J. Mol. Biol.* **94**, 425–440.

VAINSHTEIN, B. K. (1966). *Diffraction of X-rays by Chain Molecules.* Amsterdam: Elsevier.

WASER, J. (1955). *Acta Cryst.* **8**, 142–150.

Acta Cryst. (1980). A**36**, 287–295

The Physical Foundations of the Computer Simulation of X-ray Traverse Topographs

BY P. V. PETRASHEN'*

Physical-Technical Institute, Academy of Sciences of the USSR, Leningrad, USSR

F. N. CHUKHOVSKII

Institute of Crystallography, Academy of Sciences of the USSR, Moscow, USSR

AND I. L. SHULPINA

Physical-Technical Institute, Academy of Sciences of the USSR, Leningrad, USSR

(*Received* 1 *December* 1978; *accepted* 18 *October* 1979)

Abstract

A general problem of the computer simulation of X-ray traverse topographs is treated on the basis of the Green-function method. Special attention is paid to the role of partial coherence of the incident radiation and to the problem of accounting for it in the practical calculations. The reciprocity theorem for the Green functions is proved rigorously in the X-ray diffraction optics and is applied to solve the problem in question. Different approaches based on the solution of the boundary problem of the Cauchy type and on the Green-function method are analysed and are compared from the view point of the computation time needed and of their adaptation capability to real experimental conditions. It is shown that, in the present case of a small correlation length in the primary beam, the Green function method has very significant advantages, which make it the only one acceptable for practical computer

* Present address: VNII Nauch Pribor, Stakhanovtsev Street 1, 195112, Leningrad, USSR.

0567-7394/80/020287-09$01.00